



Feasibility of naphthol green-B dye adsorption using microalgae: thermodynamic and kinetic analysis

E. Gunasundari^a, P. Senthil Kumar^{a,*}, N. Rajamohan^b, Parthasarathy Vellaichamy^c

^aDepartment of Chemical Engineering, SSN College of Engineering, Chennai – 603110, India, Tel. +91 9884823425; email: senthilchem8582@gmail.com (P. Senthil Kumar), Tel. +91 9962019018; email: gunasundarielumalai2@gmail.com (E. Gunasundari)

^bChemical Engineering Section, Sohar University, Sohar, Sultanate of Oman, email: natrajmohan@gmail.com (N. Rajamohan)

^cDepartment of Physics, Hindustan Institute of Technology and Science, Chennai, Tamil Nadu, India, email: parthu0406@gmail.com (P. Vellaichamy)

Received 31 October 2019; Accepted 28 February 2020

ABSTRACT

The usage of ultrasonic-assisted *Spirulina platensis* (UASP) algal powder for the adsorption of Naphthol green-B (NGB) dye was analyzed within environmental conditions. The batch removal investigations were done with various operational conditions including UASP dose, contact time, initial NGB dye concentration and the NGB solution pH to eliminate NGB dye molecules in the aqueous solution. The optimal working conditions for the removal of NGB dye by UASP was showed that contact time (60 min), dose (3 g/L), initial NGB dye concentration (100 mg/L), pH (3), and temperature (30°C). The dye removal data were inspected by utilizing four adsorption isotherm models like Langmuir, Freundlich, Toth, and Hill isotherm models. The experimental data generated best fits within the following isotherm order: Freundlich > Hill > Toth > Langmuir isotherm model. The maximum monolayer adsorption capacity was 137.9 mg/g. The pseudo-first-order, second-order kinetic, and intraparticle diffusion models were probed and the outcomes show that the pseudo-first-order fitted with the adsorption of NGB dye molecules by UASP. Thermodynamic parameters like ΔG° , ΔH° , and ΔS° were determined and the results prove that the NGB adsorption was exothermic, spontaneous, and feasible. The results specify that the UASP has actually been utilized as an inexpensive biosorbent for the removal of NGB dye from aqueous solution.

Keywords: Naphthol green-B; *Spirulina platensis*; Equilibrium; Kinetics; Exothermic; Multilayer adsorption

1. Introduction

All over the world, water pollution is the most serious environmental problem that can be dangerous to human beings and the environment [1–4]. In general, various kinds of organic and inorganic pollutants present in wastewater that has been discharged from diverse industries for instance leather, rubber, paper, cosmetics, textile, foods, printing, wool, etc., in these; synthetic dyes are the most hazardous pollutants that may be carcinogenic, mutagenic,

or teratogenic in nature [5–11]. In the textile industry, dyeing operation can be carried out with large quantities of water and produce more volumes of colored wastewater. In this textile industry, about 1%–2% of dye losses to effluents during dye production, and 1%–10% of dye losses to effluents during dye utilization. The residual dyes in wastewater even at low quantities are common water pollutants. These dyes are generally having a complex structure that makes them toxic and not easy to decolorize even at minimum concentrations [12–15]. Thus, the rapid

* Corresponding author.

and effective treatments are needed for the elimination of synthetic dyes presented in industrial run-offs earlier being released toward water bodies. A wide variety of technologies including flocculation [16], membrane filtration [17], oxidation [18], electrolysis [19], and biological treatment methods [20] have offered and considered for their capability to eradicate dyes from wastewaters. But these technologies have more drawbacks particularly secondary sludge removal complications, higher investment, and operational expenses [21]. The dye adsorption process is shown to be an effective method to separate dye molecules from wastewaters for its simplistic design, affordable cost, easy operation method, large surface area, high adsorption capacity, chemical stability, and insensitivity toward toxic compounds. Generally, the adsorption behavior is mainly depending upon the nature of the adsorbent to be used, particularly its surface area and porosity [23,24]. In the past year, several low-cost adsorbents, such as cotton [25], corn pith [12], pine cone [26], tea leaves [27], coconut shell [28], orange peel [29], fly ash [30], peanut hull [31], wheat bran [32], etc., have been studied for the treatment of wastewater. These materials are used as adsorbent either in their raw or carbonized form. Many researchers have been reported that sulfur acid treatment was an excellent method to produce the highly carbonized form of adsorbent with increased pores and surface area [33]. In addition, the ultrasonication treatment can be further used to breakdown the functional interaction and develop new cavities with improved pore size and surface area.

The adsorbent, activated carbon (AC) is commercially utilized in order to eradicate pollutants efficiently from aqueous solutions. nevertheless, it has some drawbacks: (i) expensive and (ii) problems in its renewal. Hence, researchers are motivated to locate alternative low-cost adsorbents with excellent properties like simple production steps and the density of functional groups. Recently, microalgal biomasses have been investigated widely as feasible biosorbents to remove toxic pollutants from aqueous solutions. They comprise a significant quantity of proteins, lipids, and carbohydrates. The functional groups like carboxylate, amino, hydroxyl, phosphate, and some charged groups present in the microalgae are explained about their adsorption capacity. In recent times, some sorts of microalgae-derived biochar are prepared and used in the contaminant's removal, mainly because of their chemical composition and bio-based-product harvest [34,35]. Generally, biochar is environmentally friendly and less expensive adsorbent which is derived from waste biomass using pyrolysis. It has higher shelf-life stability, greater adsorption capacity, highly effective, and appropriate usage compare to the living algae. At the same time, more energy-intensive thermal process is needed for biochar production. The residence time and pyrolysis heating rate may possibly modify the biochar pore structure, chemical composition, and aromaticity [36].

Naphthol green-B (NGB) dye is one of the highly water-soluble anionic dye that belongs to the azoic group of dyes and is a derivative of naphthoic acid. This dye is majorly used in the solar salt industry and, textile industries for wool, nylon, and silk fabric dyeing and printing that also used for leather dyeing. The NGB dye has redox characteristics and can involve in electro-polymerization

reaction to produce steady active layers. Thus, due to its low cost and electron transfer efficiency, NGB acts as a mediator in the electrocatalysis operation especially for dopamine and uric acid and can also be used in several spectrophotometric devices [37–39]. Nowadays, the biosorption process has been used for treating dye bearing effluents due to its eco-friendly and economical nature [40]. The major goal of the current investigation is to prepare and examine the effectiveness of the ultrasonic-assisted *Spirulina platensis* (UASP) for the removal of NGB dye. The effects of numerous parameters including the NGB solution pH, UASP dose, contact time, initial NGB dye concentration, the temperature on the removal of NGB on USAP were studied. The surface morphology of UASP biosorbent was learned by using Fourier transform infrared spectroscopy (FTIR). The adsorption behavior of UASP biosorbent for the NGB dye removal was examined by using adsorption isotherm, kinetics, and mechanisms studies.

2. Materials and methods

2.1. Preparation of naphthol green-B solution

NGB dye was purchased from Loba Chemie Pvt. Ltd., Mumbai, India.

One gram of NGB dye was mixed with 1,000 mL of deionize to make 1,000 mg/L of NGB stock solution. Experimental NGB solutions were arranged through diluting the NGB stock solution using deionized water to attain the appropriate concentration of the operating solutions. The chemical structure of NGB dye is displayed in Fig. 1.

2.2. Preparation of UASP biosorbent material

Spirulina platensis microalgae were purchased from Arwind Enterprise, Vellore, Tamilnadu, India. Dust and unwanted substances present in the dried biomass were washed completely with distilled water. Then, this biomass was placed in the sunshine to dehydrate for about three days of the time period and was finely powdered. This fine powder was termed as raw *Spirulina platensis* (RSP). Then, a 1:2 weight ratio of RSP biosorbent and concentrated sulphuric acid were mixed and left for a chemical treatment to improve active size for one day. After chemical treatment, the surplus amount of acid remaining in the mixture was rinsed thoroughly using distilled water until pH = 7. After 3 h of drying (80°C), this mixture was finely milled to yield the surface-modified *Spirulina platensis* (SMSP). For the formulation of UASP biosorbent, the 3 g of SMSP fine particles and 40 mL of distilled water were assorted in a 100 mL beaker and the mix was located in the sonicator (24 kHz ultrasonic frequency) for about 1 h at 500 rpm. Later, the sonicated algal mixture was filtered through Whatman filter paper and the filtered biosorbent was dehydrated at 40°C in the oven with the drying time of 24 h. The final product was finely crushed and was labeled as UASP [41], which was performed as a biosorbent in NGB dye adsorption.

2.3. Instrumentation

The concentrations of NGB in the solutions were calculated by a UV-vis spectrophotometer (Lark LI-UV-7000,

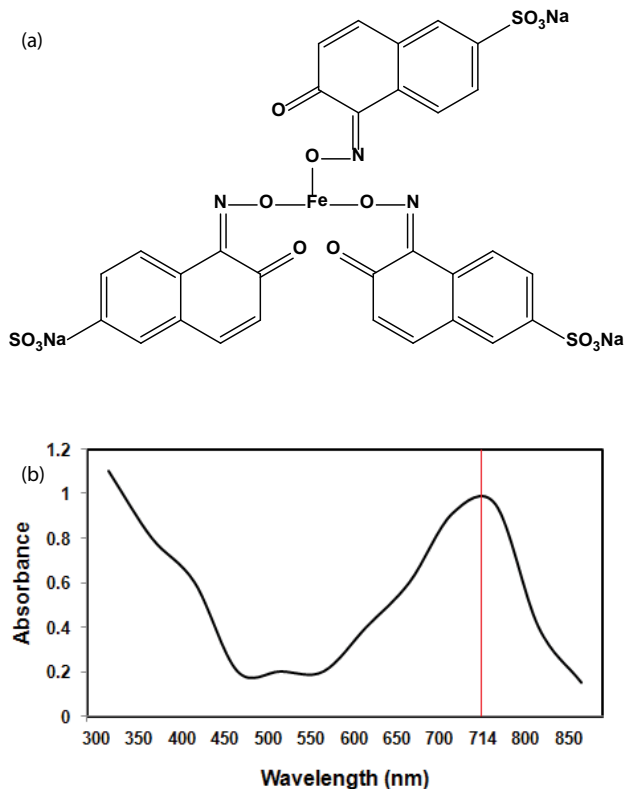


Fig. 1. (a) Chemical structure of naphthol green-B (NGB) dye and (b) UV-Vis absorption spectrum for NGB dye.

India) at 714 nm. The pH of every solution was tuned to the essential value using 0.1 M HCl or 0.1 M NaOH and was calculated with a Hanna pH meter using a combined glass electrode (Model HI9025, Singapore). FTIR spectrometer analysis was carried out using PE IR SPECTRUM ASCII PEDS 1.60 spectrometer and the spectral range is between 4,000 and 450 cm^{-1} . FTIR was used to identify the different chemical functional groups present in the UASP.

2.4. Equilibrium experiments

The experiments were implemented by taking 100 mL of NGB dye solutions in the orders of 100 mL Erlenmeyer flasks. The weighed quantity of UASP biosorbent was added into these NGB dye mixture and was stirred on temperature-controlled incubator at 80 rpm speed with dissimilar temperatures and contact time intervals. The effect of initial NGB dye concentration, UASP dose, temperature, pH, and contact time were estimated for the purpose of determining the best conditions for the NGB dye removal by UASP. Once the equilibrium achieved, the supernatant was segregated by passing through the Whatman filter paper and was further evaluated to know the remaining NGB dye concentration by UV/vis Spectrophotometer at maximum absorption wavelength (714 nm). The percentage of dye removal by algal biomass was computed using the following equation:

$$\text{NGB removal efficiency (\%)} = \frac{C_0 - C_e}{C_0} \times 100 \quad (1)$$

where C_0 is the initial NGB dye concentration in milligrams (mg) per liter (L) and C_e is the equilibrium NGB dye concentrations in milligrams (mg) per liter (L).

The amount of NGB dye uptake (q_e) was determined by the balance equation as follows:

$$q_e = \frac{(C_0 - C_e)V}{m} \quad (2)$$

where V is explicated as the volume of NGB solution (L) and m is labeled as the weight of UASP (g).

Generally, adsorption isotherm can be applied to explain the connection among dye concentration in aqueous solution and amount of dye molecules attracted onto the adsorbent material at fixed temperature per unit weight of the adsorbent material under specified conditions (pH, unchanging size, and weight of particular adsorbent). In adsorption study, a plot q_e against C_e of adsorption isotherm plays the major role to identify the region like Henry, Freundlich, and Brunauer–Emmett–Teller in there the investigational equilibrium information is absolutely placed. The capacities of adsorbent to adsorb dye molecules increase apparently with increasing the equilibrium concentration until the adsorption saturation is attained. This is assigned to the detail that greater initial dye concentration will offer greater driving force, because of which the penetration of dye onto the surface of adsorbent material will be enhanced [42]. In the present study, MATLAB R2009a software has been used to analyze Langmuir [43], Freundlich [44], Toth [45], and Hill [46] isotherm parameters by fitting the data with non-linear regression analysis.

Generally, the Langmuir isotherm model is mostly employed to explain monolayer uptake of adsorbate occurred onto the homogeneous surface of adsorbent that each molecule has constant enthalpies and adsorption activation energy without any contact among adsorbed dye molecules [47,48]. Thus, the nonlinear type of Langmuir isotherm model can be explained by Eq. (4) as follows:

$$q_e = \frac{K_L q_m C_e}{1 + C_e} \quad (3)$$

where K_L explains the Langmuir rate constant associated with the attraction between NGB dye molecules and UASP biosorbent (L/mg) and q_m is the maximum monolayer adsorption capacity of UASP biosorbent (mg/g).

Commonly, separation factor (R_L) is a non-dimensional constant that can be applied to reveal the significant feature of the Langmuir model [49] and is explained with the subsequent equation:

$$R_L = \frac{1}{1 + K_L C_0} \quad (4)$$

Based on the R_L values, the form of isotherms can be sorted as linear (in case R_L value equivalent to 1), unfavorable (in case of R_L value greater than 1), irreversible (in case R_L value equivalent to 0), and favorable (in case R_L value between 0 to 1).

Freundlich isotherm model has been utilized mainly to establish multilayer uptake that occurs onto the heterogeneous surface of the adsorbent with the interaction of

adsorbed molecules [50,51]. The non-linear form of this isotherm is generated by the following equation:

$$q_e = K_f C_e^{1/n} \quad (5)$$

where K_f indicates Freundlich constant ((mg/g) (L/mg)^(1/n)), the term n explains the deviation from linearity of sorption. When the constant n is lesser than 1 which is said to be a favorable chemical process. If the constant n is greater than 1, it is called a physical adsorption process. The adsorption becomes linear when the value n is equal to 1.

Toth isotherm model is formed by the combination of the characteristics of the Langmuir and Freundlich model. This Toth isotherm suggests asymmetrical distribution of quasi-Gaussian energy along with the majority of active sites possess lesser sorption energy compared with the highest or mean value [52,53]. This isotherm model is explained as follows:

$$q_e = \frac{f C_e}{\left[g + (C_e)^d \right]^{1/d}} \quad (6)$$

where f , g , and d are Toth isotherm constants. If the value of d is equal to 1, Toth isotherm reduces to the Langmuir isotherm, then the adsorption system is found to be homogeneous. If the constant d moves away from unity, then the process stated to be heterogeneous.

Hill isotherm model was suggested to illustrate the attachment of dissimilar adsorbate onto the surface of the homogenous adsorbent. This equation considers that the sorption process is generally called a cooperative phenomenon, besides the adsorbing substance in the one active site of adsorbent material, it can affect the several active sites of the same adsorbent material [54]. It is presented in the subsequent equation:

$$q_e = \frac{q_H C_e^{n_H} H}{K_D + C_e^{n_H} H} \quad (7)$$

where q_H is Hill isotherm maximum uptake (mg/L), n_H is Hill cooperativity coefficient of the binding interaction, and K_D is Hill constants. If the value of n_H is higher unity, this indicates positive cooperativity in binding; if the value of n_H is lesser than unity, this indicates negative cooperativity in binding; if the value of n_H is equal to unity, it implies non-cooperative or hyperbolic binding.

2.5. Kinetic experiments

The kinetics for the removal of NGB dye by using UASP biosorbent were implemented with 3 g/L of optimized UASP dose, dissimilar initial NGB dye concentrations (50–500 mg/L) and contact times (10–90 min) at optimal temperature 30°C.

The amount of adsorption at time t was ascertained by:

$$q_t = \frac{(C_0 - C_t)V}{m} \quad (8)$$

where q_t defines the quantity of NGB dye adsorbed at any time t (mg/g) and C_t is the concentration of NGB dye molecules in the solution at time t (mg/L).

In general, quite a lot of kinetic models have been offered to elucidate the adsorption kinetics. Most commonly employed kinetic models and mechanisms particularly the pseudo-first-order [55], pseudo-second-order [56], and intraparticle diffusion [57] were applied to the experimental data to estimate the biosorption kinetic of NGB dye. The best fit of these kinetic models was determined by evaluating the correlation coefficients (R^2). The effect of contact time on the removal NGB by UASP biosorbent was studied to recognize the adsorption kinetics.

The pseudo-first-order model is generally applicable to determine the adsorption rate constant [58] and is given by:

$$q_t = q_e (1 - \exp(-k_1 t)) \quad (9)$$

where k_1 is noted as the pseudo-first-order constant (min⁻¹) and t is termed as time (min).

The pseudo-second-order model, similarly pseudo-first-order model, which explains the adsorption kinetics corresponding to the chemical interaction [59] and is given by:

$$q_t = \frac{q_e^2 k_2 t}{1 + q_e k_2 t} \quad (10)$$

where k_2 is meant as the pseudo-second-order constant (g/mg min), q_t is denoted as the sorption capability of NGB dye at the period of time t (mg/g), and q_e is equilibrium sorption capability of NGB dye (mg/g).

In general, the rate-limiting steps and the adsorption mechanism were not well-discussed by adsorption kinetics including the pseudo-first-order model and the pseudo-second-order model. Thus, these has been described by Weber and Morris intraparticle diffusion model. The intraparticle diffusion model is generally plotted to check the effect of mass transfer resistance on the attachment of NGB to the UASP. The adsorption kinetics data were studied via the Weber and Morris intraparticle diffusion model to explain the diffusion mechanism and the equation is given as:

$$q_t = k_p t + C \quad (11)$$

where k_p is explained as the intraparticle diffusion rate constant (mg/g/min^{1/2}) and the term C stands for the constant associated with the boundary thickness.

2.6. Thermodynamic study

The thermodynamic investigation was conducted to comprehend about the thermodynamic parameters ΔG° (Gibb's free energy), ΔH° (enthalpy), and ΔS° (entropy). The following equations have been utilized to assess the values of thermodynamic parameters and are:

$$\Delta G^\circ = -RT \ln \left(\frac{C_{Ae}}{C_e} \right) \quad (12)$$

$$\log\left(\frac{C_{Ae}}{C_e}\right) = \frac{\Delta S^\circ}{2.3033R} - \frac{\Delta H^\circ}{2.303RT} \quad (13)$$

where the symbol T is mentioned as temperature (K), $C_{Ae}/C_e = K_e$ is referred to as the thermodynamic equilibrium constant, C_e is the NGB dye concentration in the mixture in equilibrium (mg/L), R stands for the gas constant (8.314 J/mol/K), and C_{Ae} is called as the quantity of NGB dye attracted on top of the UASP surface per liter of the mixture in equilibrium (mg/L).

3. Results and discussions

3.1. Characterization of UASP

FTIR of RSP, SMSP, and UASP (before and after NGB adsorption) was noted by using FTIR spectrometer in the wavenumber ranging from 4,000 to 400 cm^{-1} as exhibited in Fig. 2. The surface functional groups existing in the UASP as biosorbent before and after adsorption were clearly studied by FTIR characterization. The RSP spectrum displays the absorption bands at 3,282.63; 2,924.49; 1,639.21; 1,535.22; 1,397.31; 1,236.09; and 1,039.28 cm^{-1} . Two bands obtained at 3,282.63 and 2,924.49 cm^{-1} is due to the OH, primary, and secondary amine groups (stretching vibration). Three absorption peaks observed at 1,639.21; 1,535.22; and 1,397.31 cm^{-1} is due to the amide groups (bending vibration). C–N stretching of amide (or) amine groups are shown at 1,236.09 and 1,039.28 cm^{-1} . The SMSP spectrum were revealed the absorption peaks at 3,277.96; 2,920.49; 1,627.09; 1,529.96; 1,451.87; and 1,050.88 cm^{-1} . After chemical treatment, the peak at 1,397.31 cm^{-1} shifted to 1,451.87 cm^{-1} . A peak at 1,236.09 cm^{-1} was degraded. In UASP, bands were detected at 3,276.63; 2,919.42; 1,626.80; 1,531.70; 1,451.03; and 1,049.42 cm^{-1} . The peaks at 3,277.34; 2,925.20; 1,626.19; 1,518.90; and 1,031.56 cm^{-1} were found later the

removal of NGB dye by the UASP. FTIR of UASP after NGB dye adsorption as compared with UASP before NGB dye adsorption, which undoubtedly illustrates that some peak intensities were reduced, certain peaks were degraded. The results could be attained because of the attraction of the dye molecules on the active sites of the biosorbents.

3.2. Adsorption equilibrium study

In the adsorption equilibrium study, the interaction between UASP biosorbent and NGB dye along with the feasibility of various adsorption processes were determined by adsorption isotherm models at the equilibrium based on nonlinear regression of isotherm models including Langmuir, Freundlich, Toth, and Hill isotherm. Fig. 3 shows the adsorption isotherm fitting to Langmuir, Freundlich, Toth, and Hill adsorption isotherm models of NGB dye on the UASP biosorbent at 30°C, and the corresponding fitted results are listed in Table 1a. The Langmuir parameters obtained in this work are $q_m = 137.9$ mg/g, $K_L = 0.1182$ L/mg, and R^2 (correlation coefficient) = 0.8811. For the NGB dye removal, monolayer adsorption capacity (q_m) of UASP was found to be 137.9 mg/g and this was compared with various other adsorbents from literature (Table 1b). R_L values (0.458–0.144) were calculated and these values confirm the favorable NGB dye adsorption process. R_L values decreased with increasing the initial concentration of NGB dye indicating the more favorable adsorption at high concentrations. In this experiment, the Freundlich parameter n was within 1–10 because of the favorable physical NGB dye uptake process. The highly suitable adsorption isotherm model was identified by evaluating the correlation coefficient (R^2) values. The R^2 value (0.9843) of Freundlich model was quite higher than all other models including Langmuir, Toth, and Hill isotherm models, representing the greatest fit of Freundlich isotherm to the uptake of NGB dye onto

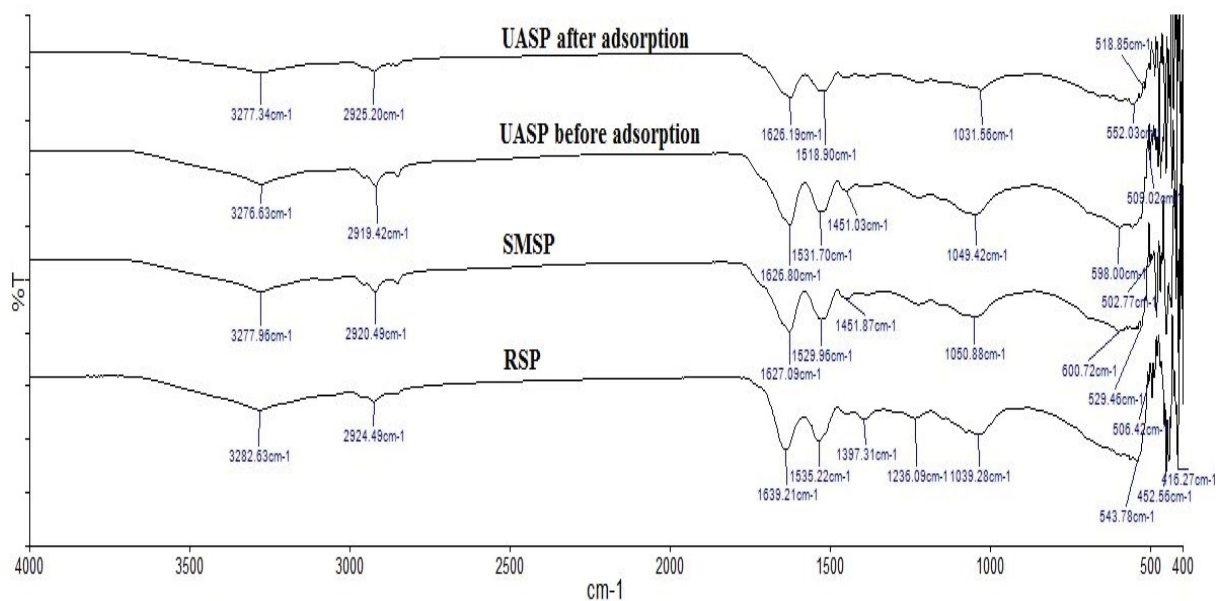


Fig. 2. Characterization of dried algal biosorbents using FTIR analysis.

UASP adsorbent. This confirms that the NGB dye sorption process is heterogeneous by its nature. Toth constant d value deviates from 1 which denotes that the isotherm fits for the modeling of the heterogeneous and multilinear adsorption

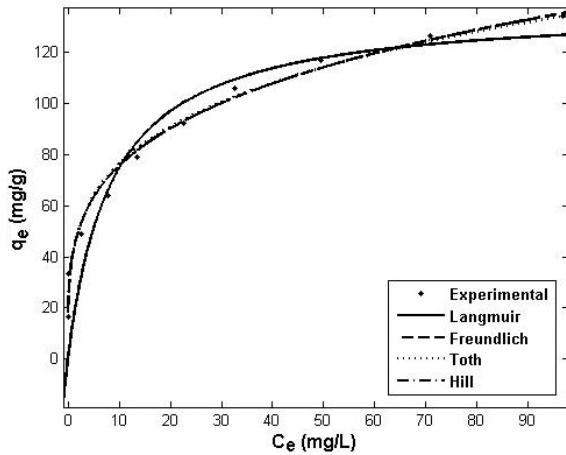


Fig. 3. Adsorption isotherm (contact time = 60 min, pH = 3.0, UASP biosorbent dose = 3 g/L, NGB dye concentration = 50–500 mg/L, and temperature 30°C).

system. The results gained from the hill isotherm model clear that the value of n_H is lesser than 1 and denotes negative cooperativity in binding.

3.3. Adsorption kinetics and mechanisms

The correlation coefficient (R^2), q_e , and rate constant (k_1 (min⁻¹) of dye under various concentration had been evaluated by using the non-linear form of plot q_t (mg/g) against time (t) (min) shown in Fig. 4 and the values are recorded in Table 2a. The gained R^2 values from the pseudo-first-order were stable and nearer to unity than from the pseudo-second-order for the adsorption of NGB dye. Further, the experimentally measured (q_e exp) and the calculated q_e values got from the pseudo-first-order kinetic model were quite similar to each other, revealing that the adsorption of NGB dye onto UASP biosorbent could be explicated in the pseudo-first-order kinetic equation.

For the intraparticle diffusion model, The parameters like C and k_p were assessed from the intercept and slope got by the linear plot between q_t and $t^{(1/2)}$ shown in Fig. 5. The correlation coefficient (R^2) and intraparticle diffusion parameters were listed in Table 2b. The intraparticle diffusion is included within the adsorption process in case the straight line obtained from the plot. In the adsorption process, it is

Table 1a
Evaluation of isotherm parameters to the NGB dye removal by UASP

Isotherm model	Parameter	R^2	SSE	RMSE
UASP scheme				
Langmuir	$q_m = 137.9$ (mg/g) $K_L = 0.1182$ (L/mg)	0.8811	1,742	14.76
Freundlich	$K_F = 41.73$ ((mg/g) (L/mg) ^(1/n)) $n = 3.886$ $f = 3.544 \times 10^5$	0.9843	230	5.362
Toth	$g = 0.3733$ $d = 0.0350$ $K_D = 445$	0.9804	287.4	6.407
Hill	$n_H = 0.2584$ $q_H = 1.861 \times 10^4$ (mg/L)	0.9842	231.5	5.751

Table 1b
Comparison of the dissimilar adsorbents adsorption capacity to remove NGB dye from aqueous solution

Adsorbent	q_m (mg/g)	References
Charcoal	232.56	[60]
Ultrasonic assisted <i>Spirulina platensis</i> (UASP)	137.9	Present study
Kaolinite	25.80	[60]
Unburned carbon 1 (UC1)	25.5	[61]
Tafla	23.86	[60]
Unburned carbon 2 (UC2)	15.2	[61]
<i>Albizia saman</i> seed shell activated carbon	11.601	[62]
Magnetic halloysite-iron oxide nanocomposite	11.2	[63]
Metal hydroxides sludge (MHS)	10	[64]
Parent coal	3	[61]

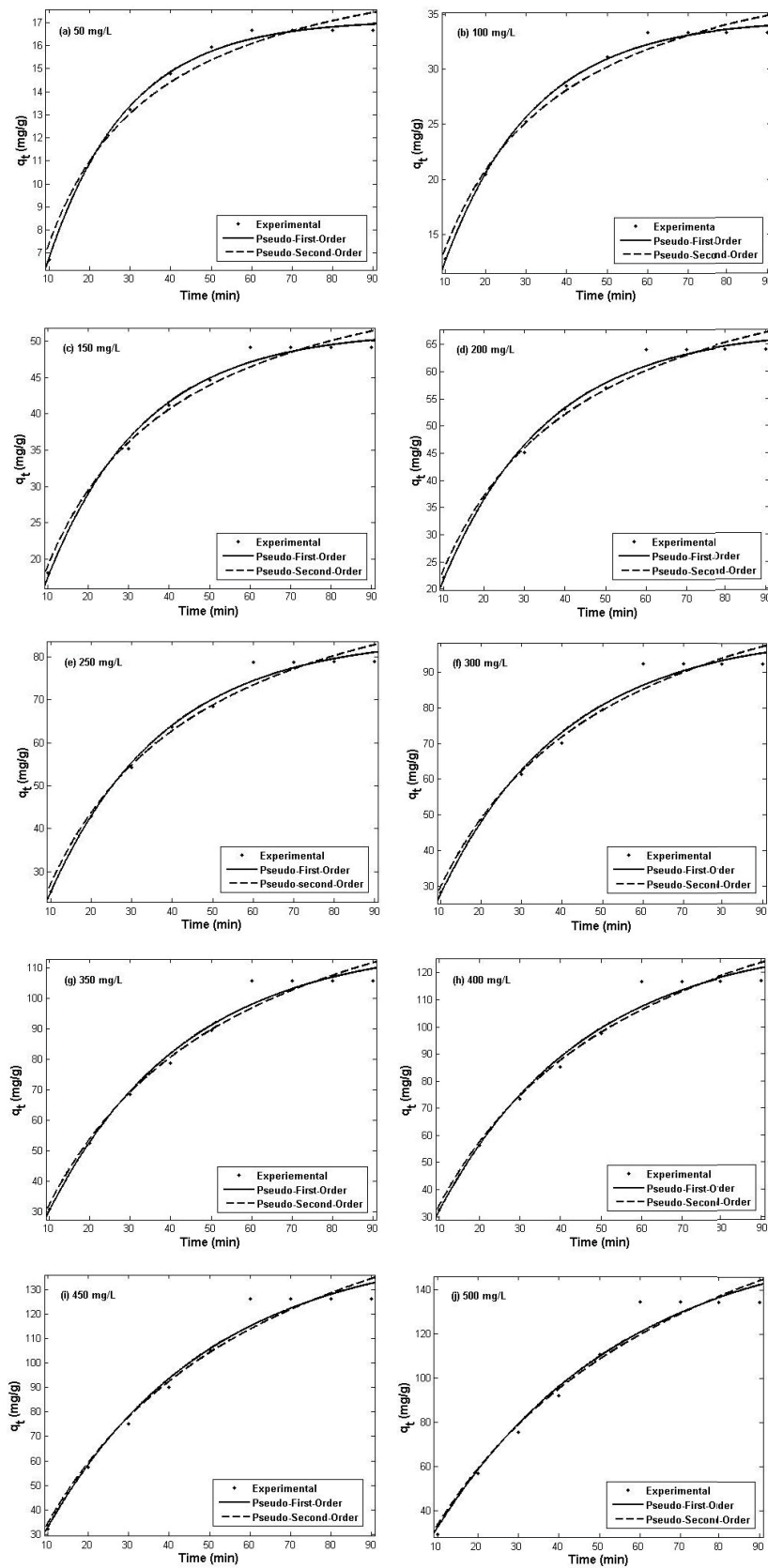


Fig. 4. Estimation of adsorption kinetics (pH = 3.0, UASP biosorbent dose = 3 g/L, NBG dye concentration = 50–500 mg/L, and temperature 30°C).

Table 2a
Adsorption kinetic for the removal of NGB dyes by UASP

C_0 (mg/L)	q_e (exp)	Pseudo-first-order			Pseudo-second-order		
		k_1 (min ⁻¹)	q_e (mg/g)	R^2	k_2 (g/mg min)	q_e (mg/g)	R^2
50	16.659	0.0507	17.1	0.9969	0.0026	20.96	0.9779
100	33.307	0.0451	34.52	0.9950	0.0010	43.2	0.9826
150	49.117	0.0415	51.35	0.9916	0.0006	65.24	0.9833
200	64.094	0.0386	67.71	0.9913	0.0004	87.4	0.9826
250	78.813	0.0353	84.56	0.9897	0.0002	111.3	0.9813
300	92.435	0.0321	101.1	0.9854	0.0002	135.7	0.9791
350	105.774	0.0295	118	0.9837	0.0001	161.5	0.9774
400	116.842	0.0277	132.7	0.9817	0.0001	184.3	0.9756
450	126.369	0.0249	148.5	0.9792	9.14e-005	212	0.9724
500	134.395	0.0216	166.2	0.9739	6.394e-005	246.3	0.9675

Table 2b
Adsorption mechanism for the removal of NGB dyes by UASP

C_0 (mg/L)	Intraparticle diffusion		
	k_p (mg/(g min ^{1/2}))	C	R^2
50	1.515	3.972	0.8668
100	3.24	5.948	0.8985
150	4.986	6.727	0.9171
200	6.776	6.318	0.9233
250	8.728	4.112	0.9311
300	10.632	0.953	0.9414
350	12.597	2.895	0.9459
400	14.262	6.468	0.9485
450	16.14	13.279	0.9469
500	18.116	22.693	0.9506

the single rate-controlling step in case the plot goes through the origin. Still, if the plot seems like the multilinear plots, either dual or extra steps effect on the NGB removal process including film diffusion, intraparticle diffusion process, etc., The dual linear plots were observed. The first part of the plot is mostly owing to the NGB dye molecules diffusion to the exterior surface of UASP biosorbent via the film and the second part is assigned to the NGB dye molecules diffusion within the pores present in UASP. The intraparticle diffusion is not a sole controlling step due to variation in the straight line in the removal of NGB dye molecules from aqueous solution using UASP biosorbent.

3.4. Impact of contact time on the elimination of NGB dye

The contact time was an important influencing factor for NGB dye adsorption process in order to find the dye removal rate. The impact of contact time on NGB dye adsorption efficiency is shown in Fig. 6. The results reveal that, the NGB dye removal increase with the expanding contact time. At first, the percentage removal of naphthol increased sharply at 60 min of contact time. Then, there is

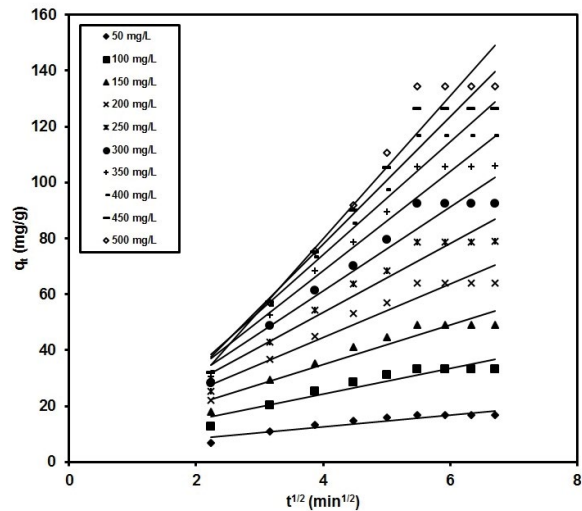


Fig. 5. Intraparticle diffusion mechanism to the NGB dye elimination.

no change in the adsorption after 60 min of contact time, that is, the percentage removal became almost constant. The dissimilarity in the adsorption rate may be as a result that the whole binding sites in the UASP surface are unoccupied and the NGB dye concentration gradient is moderately elevated. Hence, the extent of NGB dye uptake reduces with the increase of contact time, which is based on the number of unoccupied sites existing in the UASP surface.

3.5. Impact of the solution pH on adsorption of NGB dye onto UASP

The solution pH is the major factor for the dye uptake process because it influences the sorption efficiency as a result of its effect on the properties of biosorbent and adsorbate suspended in the mixture in the ionic nature. To experiment with the impact of the solution pH, the NGB dye adsorption analysis was done over a pH (2–7), and the results are shown in Fig. 7. The highest percentage of

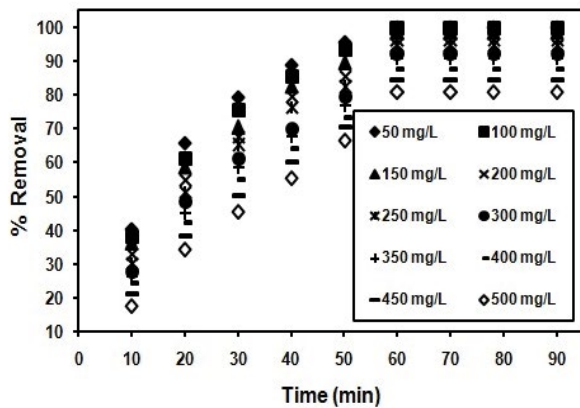


Fig. 6. Contact time influence on the NGB dye adsorption using UASP.

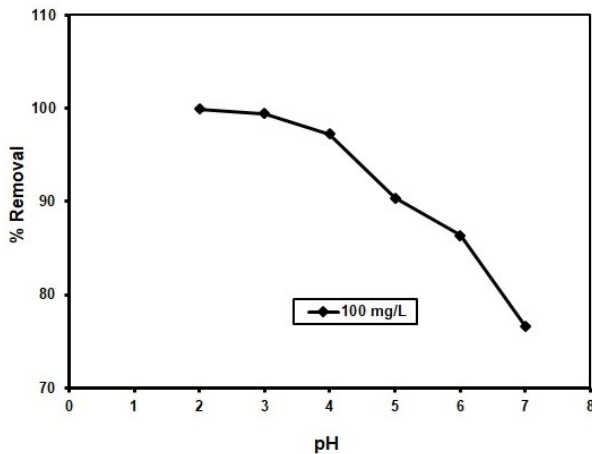
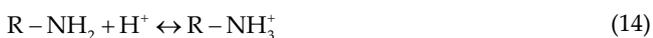


Fig. 7. pH of the solution influence on the NGB dye adsorption using UASP.

NGB dye removal reached when pH = 3 (acidic), and then, further increasing the NGB solution pH, the percentage of NGB dye removal declined. At pH = 3 (acidic), maximum electrostatic attractions take place among the UASP biosorbent (positive charge) and the anionic dye (negative charge) due to the ionization of UASP functional groups, that is, the amino groups of the UASP biosorbent were highly protonated and spread on its surface when the pH was low. These highly protonated amino groups (NH_3^+) and the negatively charged NGB dye (SO_3^-) in solution were easily bonded by the electrostatic attraction. Therefore, it leads to the greater adsorption of NGB dye on UASP. The protonation of amino groups and the adsorption of NGB dye were explained in the subsequent equations:



Besides improving the system pH, the negatively charged sites of UASP biosorbent govern over positively charged sites generating electrostatic repulsion effects, due to that the adsorption reduces [39]. Thus, the pH 3 was found to be an optimum pH for the adsorption of NGB by UASP.

3.6. Effect of amount of adsorbent dose

The influence of UASP biosorbent on the elimination of NGB dye at pH (3) is shown in Fig. 8. This adsorption experiment was carried out to see the removal percentage of NGB dye enhances through improving the UASP biosorbent quantity (0.5–3.5 g/L). The result showed the dye elimination was particularly low at the beginning. Then the percentage removal amplified with increasing the UASP biosorbent dosage. This is because; firstly, the active sites of adsorbent could not well-contact with NGB dye molecule in the aqueous solution. While increasing the adsorbent dosage from 0.5 to 3 g/L, the NGB dye removal percentage raised from 30.39% to 99.925%. Further addition of UASP biosorbent, there is no significant improvement in the adsorption of NGB dye. When the UASP dosage improved from 0.5 to 3.5 g/L, the amount NGB dye uptake reduced from 60.792 to 28.55 mg/g. Thus, the results show that the optimized quantity of adsorbent dosage (UASP) is 3 g/L at which a higher amount of NGB dyes were eliminated from aqueous solution.

3.7. Impact of initial NGB dye concentration on the adsorption processes

The impact of varying the initial NGB dye concentration from 50 to 500 mg/L, while maintaining the UASP dose (3 g/L), pH (3) and temperature of mixture (30°C) is revealed in Fig. 9. The outcomes illustrate the rate of NGB dye removal decreases from 99.96% to 80.64% by improving initial NGB dye concentration (50–500 mg/L). The lower uptake at higher NGB concentration resulted from an increased proportion of the initial quantity of NGB dye molecules in the vacant surface; therefore, fractional adsorptions become based on initial concentration. For a specified UASP biosorbent dose, the entire amount of vacant active sites in UASP biosorbent is arranged in that way attracting nearly the equal quantity of NGB adsorbate, hence resultant a decline in the NGB dye adsorption related to a rise in initial NGB dye concentration representing the total saturation of the UASP biosorbent.

3.8. Impact of temperature on NGB dye removal and thermodynamics analysis

The NGB dye adsorption on UASP was studied with initial NGB dye concentrations varying from 50 to 500 mg/L for dissimilar temperatures 30°C, 40°C, 50°C, and 60°C at pH = 3 exposed in Fig. 10. The results show that there was the reduction in NGB removal from 99.95% to 96.54%, 99.92% to 95.63%, 98.23% to 93.85%, 96.14% to 91.28%, 94.57% to 89.63%, 92.43% to 87.52%, 90.66% to 86.14%, 87.63% to 83.63%, 84.24% to 79.93%, and 80.63% to 75.63%, respectively, for the different initial NGB dye concentration (50–500 mg/L) at temperature ranging from 30°C to 60°C. This is because of

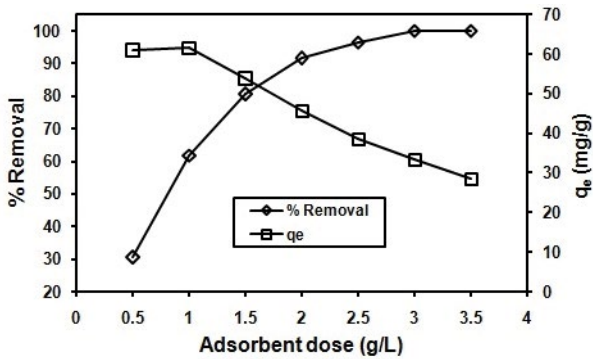


Fig. 8. UASP dose impact on the removal of NGB dye using UASP (NGB dye concentration = 100 mg/L, pH = 3.0, and temperature 30°C).

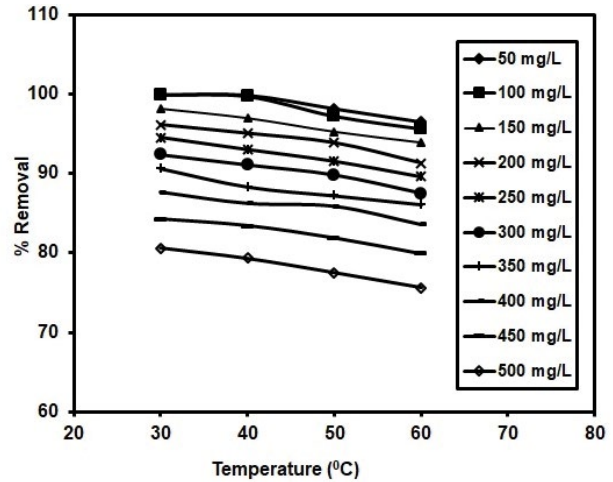


Fig. 10. Temperature impact on the NGB dye elimination using UASP.

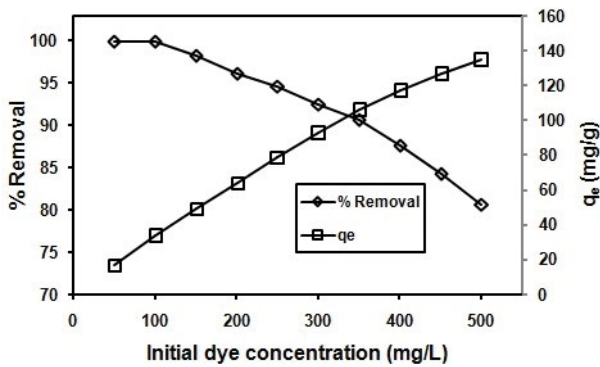


Fig. 9. Initial NGB concentration influence onto the adsorption of NGB dye onto UASP (UASP dose = 3 g/L, pH = 3.0, and temperature 30°C).

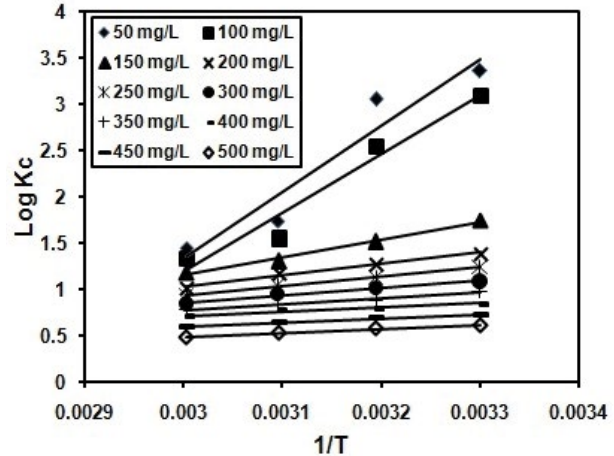


Fig. 11. Thermodynamic study on the adsorption of NGB dye onto UASP.

the fall in the surface activity. Therefore, the removal of NGB by UASP is an exothermic adsorption processes confirmed by the experimental result.

Table 3 displays the calculated K_c which decreased with increase in temperature in the NGB dye uptake by UASP biosorbent. This result clears that detachment of the adsorbed NGB dye from UASP biosorbent is greater in elevated temperature. The negative values of ΔG° explain that the adsorption process is feasible and spontaneous in nature. Fig. 11 indicates that the graph was plotted between K_c and $1/T$. The ΔH° and ΔS° values have been calculated by the slope and intercept got from the graph and are displayed in Table 3. The values of ΔH° and ΔS° were negative and confirm that the NGB sorption is an exothermic process and the declined disorderliness at UASP-NGB dye solution interface throughout the sorption of NGB dye onto UASP biosorbent.

4. Conclusion

The current investigation exposes the ability of UASP as a biosorbent for the adsorption of NGB dye from aqueous solution. FTIR spectrum results reveal that the UASP is a feasible choice for its purpose as an alternative adsorbent to eliminate NGB dye. The uptake of NGB dye present in

the water solution is mainly decided by the pH of NGB dye solution, contact time, UASP dose, temperature, and initial NGB dye molecules concentration. The percentage of NGB dye removal rises from 30.39% to 99.92% by increasing UASP dose (0.5–3 g/L) due to a corresponding improvement of active sites in UASP surface. The NGB uptake process was quick and steadiness was found within 60 min. The percentage removal of NGB dye molecules reduced with a rise in temperature (30°C–60°C). The equilibrium data obtained from the study have been checked by the four dissimilar isotherm models as Langmuir, Freundlich, Toth, and Hill isotherm models. The specific variables and R^2 values have been measured from every isotherm model. The Freundlich model is efficaciously established the uptake of NGB dye on the surface of UASP. 137.9 mg of NGB/g of UASP is the maximum monolayer adsorption capacity of UASP. Thermodynamic measures particularly ΔG° , ΔH° , and ΔS° were evaluated at different temperatures (30°C–60°C). The results showed that NGB adsorption onto UASP was observed to be exothermic and spontaneous in

Table 3
Thermodynamic parameters for adsorption of NGB dyes on UASP

C_0 (mg/L)	ΔH° (kJ/mol)	ΔS° (J/mol/K)	ΔG° (kJ/mol)			
			303 K	313 K	323 K	333 K
50	-135.92	-381.985	-19.4721	-18.2401	-10.762	-9.219
100	-121.85	-342.733	-17.9966	-15.3013	-9.568	-8.547
150	-36.705	-88.096	-10.1253	-9.0662	-8.055	-7.548
200	-23.646	-51.065	-8.1015	-7.6917	-7.323	-6.505
250	-19.376	-40.247	-7.202	-6.7533	-6.4133	-5.974
300	-15.176	-29.141	-6.306	-6.0672	-5.8591	-5.394
350	-12.173	-21.578	-5.7277	-5.2774	-5.1671	-5.0592
400	-8.447	-11.564	-4.9334	-4.7794	-4.8505	-4.517
450	-8.265	13.154	-4.2244	-4.2061	-4.0537	-3.8274
500	-8.263	-15.317	-3.5944	-3.499	-3.3255	-3.1373

nature. The adsorption kinetics of NGB onto UASP adsorbent was investigated by using different kinetic models especially the pseudo-first-order and pseudo-second-order-model. In this work, the pseudo-first-order equation offered the best correlation of the observational evidence compares to pseudo-second-order. Intraparticle diffusion mechanism was tested to learn the NGB adsorption process. Thus, it can be concluded that since the UASP is effective biosorbent and owns a significant superior adsorption potential for modeling the plant for handling the wastewater comprising NGB dye.

Symbols

C	—	Constant
C_{Ae}	—	Quantity of NGB dye attracted on top of the UASP surface per litre of mixture in equilibrium mg/L
C_0	—	Initial NGB dye concentration, mg/L
C_e	—	Equilibrium NGB dye concentrations, mg/L
C_t	—	Concentration of NGB dye molecules in the solution at time t
$^\circ C$	—	Degree Celsius
d	—	Toth isotherm constant
f	—	Toth isotherm constant
g	—	Toth isotherm constant
ΔG°	—	Gibb's free energy
ΔH°	—	Enthalpy
K_D	—	Hill constant
K_F	—	Freundlich constant, (mg/g) (L/mg) ^(1/n)
K_L	—	Langmuir rate constant, L/mg
k_p	—	Intraparticle diffusion rate constant, mg g ⁻¹ min ^{1/2}
k_1	—	Pseudo-first-order rate constant, min ⁻¹
k_2	—	Pseudo-second-order rate constant, g/mg min
M	—	Weight of UASP, g
n	—	Deviation from linearity of sorption
n_H	—	Hill cooperativity coefficient of the binding interaction
q_e	—	Amount of NGB dye uptake, mg/g
q_m	—	Maximum monolayer adsorption capacity, mg/g
q_H	—	Hill isotherm maximum uptake, mg/L

q_t	—	Quantity of NGB dye adsorbed at any time t , mg/g
R	—	Gas constant, J/mol K
R_L	—	Separation factor
ΔS°	—	Entropy
t	—	Time
V	—	Volume of NGB solution, L
%	—	Percentage

References

- [1] J.B. Neris, F.H.M. Luzardo, P.F. Santos, O.N. de Almeida, F.G. Velasco, Evaluation of single and tri-element adsorption of Pb²⁺, Ni²⁺ and Zn²⁺ ions in aqueous solution on modified water hyacinth (*Eichhornia crassipes*) fibers, *J. Environ. Chem. Eng.*, 7 (2019) 102885–102902.
- [2] P.S. Kumar, S.J. Varjani, S. Suganya, Treatment of dye wastewater using an ultrasonic aided nanoparticle stacked activated carbon: kinetic and isotherm modelling, *Bioresour. Technol.*, 250 (2018) 716–722.
- [3] C. Senthamarai, P.S. Kumar, M. Priyadarshini, P. Vijayalakshmi, V.V. Kumar, P. Baskaralingam, K.V. Thiruvengadaravi, S. Sivanesan, *Environ. Prog. Sustainable Energy*, 32 (2013) 624–632.
- [4] M.M. Hassan, C.M. Carr, A critical review on recent advancements of the removal of reactive dyes from dyehouse effluent by ion-exchange adsorbents, *Chemosphere*, 209 (2018) 201–219.
- [5] V. Tharaneedhar, P.S. Kumar, A. Saravanan, C. Ravikumar, V. Jaikumar, Prediction and interpretation of adsorption parameters for the sequestration of methylene blue dye from aqueous solution using microwave assisted corncob activated carbon, *Sustainable Mater. Technol.*, 11 (2017) 1–11.
- [6] V.V. Panic, Z.P. Madzarevic, T. Volkov-Husovic, S.J. Velickovic, Poly(methacrylic acid) based hydrogels as sorbents for removal of cationic dye basic yellow 28: kinetics, equilibrium study and image analysis, *Chem. Eng. J.*, 217 (2013) 192–204.
- [7] M. Ghaedi, A. Ansari, M.H. Habibi, A.R. Asghari, Removal of malachite green from aqueous solution by zinc oxide nanoparticle loaded on activated carbon: kinetics and isotherm study, *J. Ind. Eng. Chem.*, 20 (2014) 17–28.
- [8] S. Suganya, P.S. Kumar, A. Saravanan, P.S. Rajan, C. Ravikumar, Computation of adsorption parameters for the removal of dye from wastewater by microwave assisted sawdust: theoretical and experimental analysis, *Environ. Toxicol. Pharmacol.*, 50 (2017) 45–57.
- [9] L. Huang, M. He, B. Chen, B. Hu, Magnetic Zr-MOFs nanocomposites for rapid removal of heavy metal ions and dyes from water, *Chemosphere*, 199 (2018) 435–444.

- [10] P. SenthilKumar, N. Umayambika, R. Gayathri, Dye removal from aqueous solution by electrocoagulation process using stainless steel electrodes, *Environ. Eng. Manage. J.*, 9 (2010) 1031–1037.
- [11] Z.U. Ahmad, L. Yao, J. Wang, D.D. Gang, F. Islam, Q. Lian, M.E. Zappi, Synthesis and characterization of novel functionalized ordered mesoporous carbon (omc) for resorcinol and sunset yellow removal, *Chem. Eng. J.*, 359 (2019) 814–826.
- [12] R. Jothirani, P.S. Kumar, A. Saravanan, A.S. Narayan, A. Dutta, Ultrasonic modified corn pith for the sequestration of dye from aqueous solution, *J. Ind. Eng. Chem.*, 39 (2016) 162–175.
- [13] G.K. Devi, P.S. Kumar, K.S. Kumar, Green synthesis of novel silver nanocomposite hydrogel based on sodium alginate as an efficient biosorbent for the dye wastewater treatment: prediction of isotherm and kinetic parameters, *Desal. Water Treat.*, 57 (2016) 27686–27699.
- [14] D. Sivakumar, R. Parthiban, P.S. Kumar, Synthesis and characterization of ultrasonic-assisted *Delonix regia* seeds: modelling and application in dye adsorption, *Desal. Water Treat.*, 173 (2020) 427–441.
- [15] N.R. de Mattos, C.R. de Oliveira, L.G.B. Camargo, R.S.R. da Silva, R.L. Lavall, Azo dye adsorption on anthracite: a view of thermodynamics, kinetics and cosmotropic effects, *Sep. Purif. Technol.*, 209 (2019) 806–814.
- [16] S.S. Moghaddam, M.R.A. Moghaddam, M. Arami, Coagulation/flocculation process for dye removal using sludge from water treatment plant: optimization through response surface methodology, *J. Hazard. Mater.*, 175 (2010) 651–657.
- [17] P. Shi, X. Hu, Y. Wang, M. Duan, S. Fang, W. Chen, A PEG-tannic acid decorated microfiltration membrane for the fast removal of Rhodamine B from water, *Sep. Purif. Technol.*, 207 (2018) 443–450.
- [18] P.V. Nidheesh, M. Zhou, M.A. Oturan, An overview on the removal of synthetic dyes from water by electrochemical advanced oxidation processes, *Chemosphere*, 197 (2018) 210–227.
- [19] Y. Han, H. Li, M. Liu, Y. Sang, C. Liang, J. Chen, Purification treatment of dyes wastewater with a novel micro-electrolysis reactor, *Sep. Purif. Technol.*, 170 (2016) 241–247.
- [20] D. Bhatia, N.R. Sharma, J. Singh, R.S. Kanwar, Biological methods for textile dye removal from wastewater: a review, *Crit. Rev. Environ. Sci. Technol.*, 47 (2017) 1836–1876.
- [21] Y. Zhao, Y. Chen, J. Zhao, Z. Tong, S. Jin, Preparation of SA-g-(PAA-co-PDMS) polyampholytic superabsorbent polymer and its application to the anionic dye adsorption removal from effluents, *Sep. Purif. Technol.*, 188 (2017) 329–340.
- [22] J. Perez-Calderon, M.V. Santos, N. Zaritzky, Reactive RED 195 dye removal using chitosan coacervated particles as bio-sorbent: analysis of kinetics, equilibrium and adsorption mechanisms, *J. Environ. Chem. Eng.*, 6 (2018) 6749–6760.
- [23] A. Oussalah, A. Boukerroui, A. Aichour, B. Djellouli, Cationic and anionic dyes removal by low-cost hybrid alginate/natural bentonite composite beads: adsorption and reusability studies, *Int. J. Biol. Macromol.*, 124 (2019) 854–862.
- [24] M. Ertas, B. Acemioglu, M.H. Alma, M. Usta, Removal of methylene blue from aqueous solution using cotton stalk, cotton waste and cotton dust, *J. Hazard. Mater.*, 183 (2010) 421–427.
- [25] N.M. Mahmoodi, B. Hayati, M. Arami, C. Lan, Adsorption of textile dyes on pine cone from colored wastewater: kinetic, equilibrium and thermodynamic studies, *Desalination*, 268 (2011) 117–125.
- [26] M. Foroughi-Dahr, H. Abolghasemi, M. Esmaili, A. Shojamoradi, H. Fatoorehchi, Adsorption characteristics of Congo red from aqueous solution onto tea waste, *Chem. Eng. Commun.*, 202 (2015) 181–193.
- [27] M.A. Acheampong, K. Pakshirajan, A.P. Annachatre, P.N.L. Lens, Removal of Cu(II) by biosorption onto coconut shell in fixed-bed column systems, *J. Ind. Eng. Chem.*, 19 (2013) 841–848.
- [28] S. Hashemian, K. Salari, Z.A. Yazdi, Preparation of activated carbon from agricultural wastes (almond shell and orange peel) for adsorption of 2-pic from aqueous solution, *J. Ind. Eng. Chem.*, 20 (2014) 1892–1900.
- [29] M. Arami, N.Y. Limaee, N.M. Mahmoodi, N.S. Tabrizi, Removal of dyes from colored textile wastewater by orange peel adsorbent: equilibrium and kinetic studies, *J. Colloid Interface Sci.*, 288 (2005) 371–376.
- [30] S. Wang, Y. Boyjoo, A. Choueib, A comparative study of dye removal using fly ash treated by different methods, *Chemosphere*, 60 (2005) 1401–1407.
- [31] N. Tahir, H.N. Bhatti, M. Iqbal, S. Noreen, Biopolymers composites with peanut hull waste biomass and application for Crystal Violet adsorption, *Int. J. Biol. Macromol.*, 94 (2017) 210–220.
- [32] M.T. Sulak, H.C. Yatmaz, Removal of textile dyes from aqueous solutions with eco-friendly biosorbent, *Desal. Water Treat.*, 37 (2012) 169–177.
- [33] S. Karagoz, T. Tay, S. Ucar, M. Erdem, Activated carbons from waste biomass by sulfuric acid activation and their use on methylene blue adsorption, *Bioresour. Technol.*, 99 (2008) 6214–6222.
- [34] S. Biswas, T.K. Sen, A.M. Yeneneh, B.C. Meikap, Synthesis and characterization of a novel Ca-alginate-biochar composite as efficient zinc (Zn^{2+}) adsorbent: thermodynamics, process design, mass transfer and isotherm modeling, *Sep. Sci. Technol.*, 54 (2019) 1106–1124.
- [35] Y.K. Choi, T.R. Choi, R. Gurav, S.K. Bhatia, Y.L. Park, H.J. Kim, E. Kan, Y.H. Yanga, Adsorption behavior of tetracycline onto *Spirulina* sp. (microalgae)-derived biochars produced at different temperatures, *Sci. Total Environ.*, 210 (2020) 136282–136291.
- [36] H. Zheng, W. Guo, S. Li, Y. Chen, Q. Wua, X. Feng, R. Yin, S. Ho, N. Ren, J. Chang, Adsorption of p-nitrophenols (PNP) on microalgal biochar: analysis of high adsorption capacity and mechanism, *Bioresour. Technol.*, 244 (2017) 1456–1464.
- [37] B.H. Hameed, A.A. Ahmad, Batch adsorption of methylene blue from aqueous solution by garlic peel, an agricultural waste biomass, *J. Hazard. Mater.*, 164 (2009) 870–875.
- [38] F. Zhang, Z. Ni, S. Xia, X. Liu, Q. Wang, Removal of naphthol green B from aqueous solution by calcined layered double hydroxides: adsorption property and mechanism studies, *Chin. J. Chem.*, 27 (2009) 1767–1772.
- [39] S. Dawood, T.K. Sen, Removal of anionic dye Congo red from aqueous solution by raw pine and acid-treated pine cone powder as adsorbent: equilibrium, thermodynamic, kinetics, mechanism and process design, *Water Res.*, 46 (2012) 1933–1946.
- [40] Z. Li, X. Meng, Z. Zhang, Equilibrium and kinetic modelling of adsorption of Rhodamine B on MoS_2 , *Mater. Res. Bull.*, 111 (2019) 238–244.
- [41] E. Gunasundari, P.S. Kumar, Higher adsorption capacity of *Spirulina platensis* alga for Cr(VI) ions removal: parameter optimisation, equilibrium, kinetic and thermodynamic predictions, *IET Nanobiotechnol.*, 11 (2017) 317–328.
- [42] B.H. Hameed, A.T.M. Din, A.L. Ahmad, Adsorption of methylene blue onto bamboo-based activated carbon: kinetics and equilibrium studies, *J. Hazard. Mater.*, 141 (2007) 819–825.
- [43] I. Langmuir, The adsorption of gases on plane surfaces of glass, mica and platinum, *J. Am. Chem. Soc.*, 40 (1918) 1361–1403.
- [44] H.M.F. Freundlich, Over the adsorption in solution, *J. Phys. Chem.*, 57 (1906) 385–471.
- [45] J. Toth, State equations of the solid-gas interface layers, *Acta Chim. Acad. Sci. Hung.*, 69 (1961) 311–317.
- [46] A. Khan, R. Ataullah, A. Al-Haddad, Equilibrium adsorption studies of some aromatic pollutants from dilute aqueous solutions on activated carbon at different temperature, *J. Colloid Interface Sci.*, 194 (1997) 154–165.
- [47] Z. Al-Qodah, M. Al-Shannag, Heavy metal ions removal from wastewater using electrocoagulation processes: a comprehensive review, *Sep. Sci. Technol.*, 52 (2017) 2649–2676.
- [48] K. Gayathri, N. Palanisamy, Methylene blue adsorption onto an eco-friendly modified polyacrylamide/graphite composites: investigation of kinetics, equilibrium, and thermodynamic studies, *Sep. Sci. Technol.*, 55 (2020) 266–277.
- [49] T.W. Weber, R.K. Chakraborty, Pore and solid diffusion models for fixed bed adsorbents, *AIChE J.*, 20 (1974) 228–238.

- [50] R.A. Raj, V. Manimozhi, R. Saravanathamizhan, Adsorption studies on removal of Congo red dye from aqueous solution using petroleum coke, *Pet. Sci. Technol.*, 37 (2019) 913–924.
- [51] C. Manera, A.P. Tonello, D. Perondi, M. Godinho, Adsorption of leather dyes on activated carbon from leather shaving wastes: kinetics, equilibrium and thermodynamics studies, *Environ. Technol.*, 40 (2019) 2756–2768.
- [52] Nasruddin, A. Martin, M.I. Alhamid, D. Tampubolon, Adsorption isotherms of hydrogen on granular activated carbon derived from coal and derived from coconut shell, *Heat Transfer Eng.*, 38 (2017) 403–408.
- [53] R. Ramadoss, D. Subramaniam, Removal of divalent nickel from aqueous solution using blue-green marine algae: adsorption modeling and applicability of various isotherm models, *Sep. Sci. Technol.*, 54 (2019) 943–961.
- [54] N.S. Yousef, R. Farouq, R. Hazzaa, Adsorption kinetics and isotherms for the removal of nickel ions from aqueous solutions by an ion-exchange resin: application of two and three parameter isotherm models, *Desal. Water Treat.*, 57 (2016) 21925–21938.
- [55] S. Lagergren, About the theory of so-called adsorption of soluble substances, *Kungl. Svenska Vetenskapsakad. Handl.*, 24 (1898) 1–39.
- [56] Y.S. Ho, G. McKay, Pseudo-second order model for sorption processes, *Process Biochem.*, 34 (1999) 451–465.
- [57] W.J. Weber, J.C. Morris, Kinetics of adsorption on carbon from solution, *J. Sanit. Eng. Div.*, 89 (1963) 31–60.
- [58] İ. Özbay, U. Özdemir, B. Özbay, S. Veli, Kinetic, thermodynamic, and equilibrium studies for adsorption of azo reactive dye onto a novel waste adsorbent: charcoal ash, *Desal. Water. Treat.*, 51 (2013) 6091–6100.
- [59] A.M.A. Ali, R.K. Kathikeyan, M.S. Selvan, M.K. Rai, M. Priyadharshini, N. Maheswari, G.J. Sree, V.C. Padmanaban, R.S. Singh, Removal of Reactive Orange 16 by adsorption onto activated carbon prepared from rice husk ash: statistical modelling and adsorption kinetics, *Sep. Sci. Technol.*, 55 (2020) 26–34.
- [60] S.E. Rizk, M.M. Hamed, Batch sorption of iron complex dye, naphthol green B, from wastewater on charcoal, kaolinite, and tafla, *Desal. Water Treat.*, 56 (2015) 1536–1546.
- [61] L. Bartonova, L. Ruppenthalova, M. Ritz, Adsorption of Naphthol Green B on unburned carbon: 2-and 3-parameter linear and non-linear equilibrium modelling, *Chin. J. Chem. Eng.*, 25 (2017) 37–44.
- [62] M. Rajeswari, K. Arivalagan, S. Sivanesan, R. Tamilarasan, Modeling studies for the removal of Naphthol Green B from aqueous solution using *Albizia saman* seed shell activated carbon, *Int. J. Innovative Res. Sci. Technol.*, 4 (2017) 142–148.
- [63] R. Riahi-Madvaar, M.A. Taher, H. Fazelirad, Synthesis and characterization of magnetic halloysite-iron oxide nanocomposite and its application for naphthol green B removal, *Appl. Clay. Sci.*, 137 (2017) 101–106.
- [64] M.F. Attallah, I.M. Ahmed, M.M. Hamed, Treatment of industrial wastewater containing Congo red and Naphthol green B using low-cost adsorbent, *Environ. Sci. Pollut. Res.*, 20 (2013) 1106–1116.